ISSN 1070-3632, Russian Journal of General Chemistry, 2016, Vol. 86, No. 4, pp. 901–906. © Pleiades Publishing, Ltd., 2016.

Transition Metal Chelates: Synthesis, Physicochemical, Thermal, and Biological Studies[1]

N. J. Suryawanshi[a], G. B. Pethe[b], A. R. Yaul[b], and A. S. Aswar[b]

[a] *Department of Industrial Chemistry, Arts, Science and Com. College, Chikhaldara, 444807 India*
e-mail: aswar2341@rediffmail.com

[b] *Department of Chemistry, Sant Gadge Baba Amravati University, Amravati, 444602 India*

Received May 10, 2015

Abstract—The transition metal complex of Mn(II), Co(II), Ni(II), Cu(II), Ti(III), Cr(III), Fe(III), Zr(IV), and UO_2(VI) ion with a Schiff's base ligand derived from 2-hydroxy-[2-oxo-1,2-dihydro-3*H*-indol-3-ylidene]-benzohydrazide have been prepared. The complexes have been characterized by elemental analysis data, IR and electronic absorption spectra, magnetic moments, and thermogravimetric analysis data. The complexes of the 1 : 1 metal-to-ligand stoichiometry have been formed. The physico-chemical data have suggested the octahedral geometry for all the complexes except for Cu(II); the Cu(II) complex has been square planar. Thermal analysis data of the ligand and its complexes have been analyzed, and the kinetic parameters have been determined using the Horowitz–Metzger method. According to the solid-state electrical conductivity measurements, the ligand and its complexes are semiconducting in nature. The antimicrobial activity of the ligand and the complexes towards *E. coli, S. typhi, P. aeruginosa*, and *S. aureus* has been tested by the disc diffusion method.

Keywords: hydrazone, Schiff's base, thermal analysis, electrical conductivity, antimicrobial activity, scanning electron microscopy

DOI: 10.1134/S1070363216040241

Studies of the Schiff's bases and their metal complexes have contributed much to the development of coordination chemistry. These compounds are of special importance in view of diverse applications in various branches of modern applied chemistry. Transition metal complexes of hydrazones of the Schiff's bases have been among the most widely studied coordination compounds over the past few decades. The coordination chemistry of transition metal complexes of hydrazones has been intensively investigated due to their biological activity [1] giving rise to their application in the treatment of tuberculosis [2], mental disorders, and tumors [3, 4]; on top of that, they are also known as herbicides and insecticides [5]. Hydrazones have been recognized as analytical reagents for determination of metal ions [6, 7]. In the view of the importance of hydrazones, in this work we prepared the Schiff's base of 2-hydroxy-1-(2-hydroxy-5-methyl-3-nitrophenyl)ethylidene]benzohydrazide and studied its complexes with Mn(II), Co(II), Ni(II), Cu(II), Ti(III), Cr(III), Fe(III), Zr(IV), and UO_2(VI).

The complexes were colored solids stable in air and insoluble in water as well as in most of the common organic solvents. The physico-chemical data including elemental analysis results, color, electrical conductivity, and activation energy of the compounds decomposition are collected in Table 1. The results indicated the formation of the 1 : 1 (metal : ligand) stoichiometry for all the complexes.

IR spectra of the complexes were compared with that of the free ligand. The free ligand spectrum contained a band at 1710 cm^{-1} assigned to the ν(C=O) mode of the isatin moiety and of the hydrazone amide group [8]. The band due to the ν(C=N) vibration appeared at 1639 cm^{-1}. The isatin ν(C=O) band of the complexes was shifted towards lower frequency by 9–22 cm^{-1} due to the coordination of the C=O group at the metal ion. The ν(C=N) band was shifted to lower frequencies by 10–32 cm^{-1}, thus indicating the coordination of azomethine nitrogen at the metal ion. A broad band observed at 3260 cm^{-1} was assigned to the hydroxyl group of isatin involved in the intramolecular hydrogen bonding with the NH group. The amide ν(C=O) band was absent in the spectra of all the complexes, and a new band of the ν(C–O) appeared at

[1] The text was submitted by the authors in English.

Table 1. Analytical data of ligand and its complexes

Compound	Color	Elemental analysis, wt %								Electrical conductivity, Ω^{-1} cm^{-1}	Activation energy, eV
		found				calculated					
		M	C	H	N	M	C	H	N		
L	Orange	–	64.22	4.02	14.75	–	64.05	3.94	14.94	–	–
$[Mn(L)Cl·H_2O]_2$	Black-brown	14.03	46.18	3.02	10.76	14.14	46.36	3.11	10.81	4.36×10^{-10}	0.178
$[Co(L)Cl·H_2O]_2$	Greenish red	14.87	45.76	3.01	10.62	14.87	45.88	3.08	10.70	5.88×10^{-9}	0.220
$[Ni(L)Cl·2H_2O]$	Dark gray	10.11	43.75	3.19	10.16	10.24	43.89	3.44	10.24	3.89×10^{-11}	0.150
$[Cu(L)]Cl_2$	Greenish brown	16.58	47.37	2.54	10.97	16.76	47.50	2.66	11.08	1.31×10^{-12}	0.084
$[Ti(L)Cl_2·H_2O]$	Pale yellow	11.36	43.11	2.83	9.95	11.48	43.20	2.90	10.08	4.67×10^{-11}	0.327
$[Cr(L)Cl_2·H_2O]$	Dark brown	16.78	42.65	2.70	9.81	16.84	42.78	2.87	9.98	2.18×10^{-12}	0.193
$[Fe(L)Cl_2·H_2O]$	Olive brown	13.03	42.27	2.74	8.75	13.03	42.39	2.85	9.89	1.12×10^{-10}	0.330
$[Zr(OH)_3(L)CH_3OH]$	Musk yellow	18.58	44.15	3.17	9.54	18.63	44.18	3.26	9.67	5.62×10^{-9}	0.204
$[UO_2(L)CH_3OH]NO_3$	Reddish yellow	33.85	29.74	2.10	8.56	36.94	29.82	2.19	8.70	1.20×10^{-12}	0.110

1092–1120 cm^{-1}, evidencing about enolization of the carbonyl group in the course of the complex formation. Furthermore, IR spectra of the metal complexes lacked the ν(NH) absorption band, but exhibited a strong band at 1607–1629 cm^{-1} due to the vibrations of the –C=N–N=C– moiety [9]. Hence, the ligand likely acted as a singly-charged tridentate chelating agent coordinated at the central metal ion via azomethine nitrogen, the enol oxygen, and the isatin carbonyl oxygen atoms. The spectra of uranyl and Zr(IV) complexes contained a band at ≈950 cm^{-1} due to the presence of methanol, and the band observed at 927 cm^{-1} in the spectrum of the uranyl complex was assigned to the ν_{as}(O=U=O) mode [10–12]. The coordination of H_2O in the Mn(II), Co(II), Ni(II), Ti(III), Cr(III), and Fe(III) complexes was indicated by the appearance of the absorption bands at 3218–3356 [ν(OH)], 1502–1547 [δ(H_2O)], and 806–842 [ρ(H_2O)] cm^{-1}. In addition to above bands, all the complexes showed the absorption bands in the far-infrared region: 502–557 [ν(M–O)] and 442–490 [ν(M–N)] cm^{-1} [13].

The electronic absorption spectral data and magnetic moment values were further studied to determine the complexes geometry. In particular, the Mn(II) complex exhibited three bands at 17482, 24213, and 26954 cm^{-1}, assigned to the $^6A_{1g}\rightarrow{}^4T_{1g}(^4G)$, $^6A_{1g}\rightarrow{}^4T_{2g}(^4G)$, and $^6A_{1g}\rightarrow{}^4E_g$, transitions, respectively. The electronic absorption spectral and the determined magnetic moment of 6.02 μ_B suggested the octahedral geometry of the Mn(II) ion [14, 15]. The Co(II) complex exhibited three peaks at 10309, 16286, and 24154 cm^{-1}, assigned to the $^4T_{1g}(F)\rightarrow{}^4T_{2g}(F)$, $^4T_{1g}(F)\rightarrow{}^4T_{1g}(P)$, and $^4T_{1g}(F)\rightarrow{}^4A_{2g}(F)$ transitions, respectively; that was indicative of the octahedral environment of the central Co(II) ion [16]. The ligand field parameters of the metal–ligand bond in the Co(II) complex were determined [Δq of 548 cm^{-1}, the Racah interelectronic repulsion parameter (β') of 634 cm^{-1}, the nephelauxetic ratio (β) of 0.65, and ν_1/ν_2 of 1.57]. The Racah inter-electronic repulsion parameter for the complex was lower than that for the free ion (971 cm^{-1}), suggesting delocalization of the metal electron over the metal and the ligand i.e. the significant covalent character in the metal–ligand bond. The magnetic moment value for the Co(II) complex was of 4.82 μ_B, suggesting the high-spin octahedral type complex type. The Ni(II) complex exhibited three spectral bands at 10559, 17006, and 26246 cm^{-1} corresponding to the $^3A_{2g}(F)\rightarrow{}^3T_{2g}(F)$, $^3A_{2g}(F)\rightarrow{}^3T_{1g}(F)$, and $^3A_{2g}(P)\rightarrow{}^3T_{1g}(P)$ transitions, respectively, revealing the octahedral geometry around Ni(II) ion [17]. The ligand field parameters of the metal–ligand bond in the latter complex were determined [Δq of 1055.9 cm^{-1}, the Racah inter-electronic repulsion parameter (β') of 771.66 cm^{-1}, the nephelauxetic ratio (β) of 0.74, and ν_1/ν_2 of 1.61], the

fraction of the covalent character of the bond being of 25.23%. The Racah inter-electronic repulsion parameter for the complex was again lower than that for the free ion, suggesting the electron density delocalization between the metal ion and the ligand. The ν_1/ν_2 ratio was in the range of the octahedral Ni(II) complexes. The magnetic moment value for the Ni(II) complex was of 3.13 μ_B, suggesting the octahedral surrounding of the metal ion. The Cu(II) complex showed three bands at 15267, 17214, and 19920 cm^{-1} corresponding to the $^2B_{1g}\rightarrow{}^2A_{1g}$, $^2B_{1g}\rightarrow{}^2E_g$, and charge transfer transitions, respectively, evidencing about the square planar Cu(II) complex geometry [18]. The magnetic moment value of Cu(II) complex was of 1.30 μ_B. The unusual magnetic moment value might be owing to the metal–metal interaction in the dimeric structure. The Ti(III) complex showed a broad band at 18315 cm^{-1} likely related to the $^2T_{2g}\rightarrow{}^2E_g$ transition of the octahedral geometry of the Ti(III) ion. The magnetic moment of the Ti(III) complex was of 1.62 μ_B, corresponding to one unpaired electron in the octahedral surrounding of the ion. The Cr(III) complex exhibited three characteristic bands at 18115 cm^{-1} (ν_1), 24449 cm^{-1} (ν_2), and 38910 cm^{-1} (ν_3) assigned to the $^4A_{2g}(F)\rightarrow{}^4T_{2g}(F)$, $^4A_{2g}(F)\rightarrow{}^4T_{1g}(F)$, and $^4A_{2g}(F)\rightarrow{}^4T_{1g}(P)$ transitions, respectively. The ligand field parameters of the metal–ligand bond in the latter complex were determined [Δq of 1811 cm^{-1}, the Racah inter-electronic repulsion parameter (β') of 600 cm^{-1}, the nephelauxetic ratio (β) of 0.652, and ν_1/ν_2 of 1.35], the fraction of the covalent character of the bond being of 3.48%. The Racah inter-electronic repulsion parameter for the complex was again lower than that for the free ion, suggesting the electron density delocalization between the metal ion and the ligand [19].The ν_2/ν_1 ratio of 1.34 was very close to the value of 1.42 obtained for the purely octahedral Cr(III) complexes [20, 21]. The magnetic moment value of 3.94 μ_B further evidenced about the octahedral geometry of the Cr(III) ion [22]. The Fe(III) complex exhibited three spectral bands at 13679, 17857, and 22883 cm^{-1} assigned to the $^6A_{1g}\rightarrow{}^4T_{1g}(G)$, $^6A_{1g}\rightarrow{}^4T_{2g}(G)$, and $^6A_{1g}\rightarrow{}^4E_g$, $^4T_{1g}(G)$, transitions, respectively, corresponding to the octahedral geometry around Fe(III) ion [23]. The magnetic moment was of 5.88 μ_B, indicating high-spin state of the complex. The Zr(IV) and UO_2^{2+} complexes were diamagnetic, as expected from their electronic configuration [24].

In order to investigate the stability of the complexes, the TG analysis was carried out; the basic results are shown in Fig. 1. The TG curves revealed three-stage decomposition pattern for the Mn(II), Co(II), Ni(II), Ti(III), Cr(III), and Fe(III) complexes and two-stage decomposition in the case of the free ligand as well as the Cu(II), Zr(IV), and UO_2^{2+} complexes. The mass loss corresponding to two [the Mn(II), Co(II), and Ni(II) complexes] or one [Ti(III), Cr(III), and Fe(III) complexes] coordinated water molecules was observed in the first step (160–210°C) [the observed/calculated mass loss was of 4.80/4.63, Mn(II); 4.67/4.58 Co(II); 8.92/8.77, Ni(II); 4.19/4.31, Ti(III); 4.39/4.27, Cr(III); 4.37/4.23, Fe(III) (wt %)]. The Ti(III), Cr(III), and Fe(III) complexes were stable up to 290°C, showing gradual weight loss at further heating up to ≈470°C, corresponding to the loss of the coordinated ligand [25]. The Ti(III), Cr(III) and Fe(III) complexes were almost stable up to 220°C, indicating the absence of lattice or coordinated water molecules. In the cases of Mn(II), Co(II), Ni(II), Cu(II), Ti(III), Cr(III), and Fe(III) complexes, rapid mass loss was observed over 290–470°C, assigned to the loss of the organic part of the coordinated ligand. Further heating was accompanied by gradual weight loss corresponding to the decomposition of the remaining part of

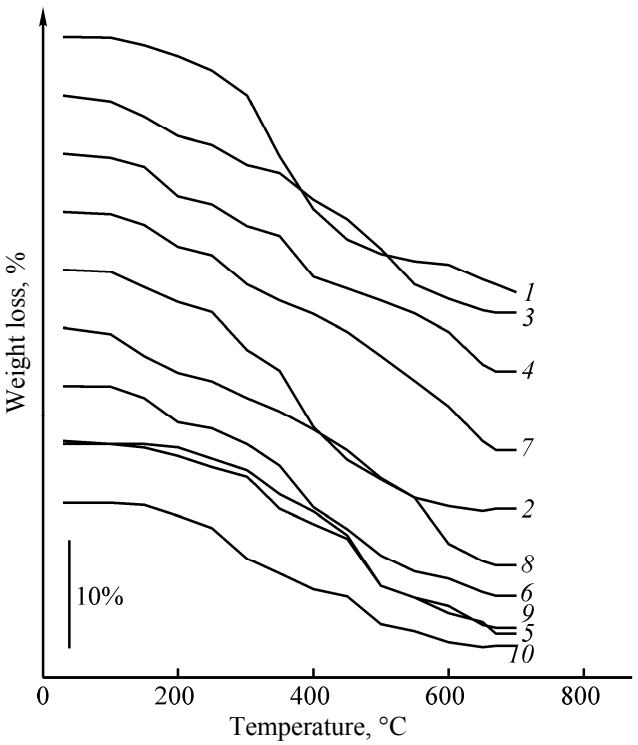

Fig. 1. Thermograms of the ligand and its complexes. (*1*) Ligand, (*2*) Mn(II), (*3*) Co(II), (*4*) Ni(II), (*5*) Cu(II), (*6*) Ti(III), (*7*) Cr(III), (*8*) Fe(III), (*9*) Zr(IV), and (*10*) UO_2(VI).

Table 2. Thermal decomposition data of ligand and its complexes

Compound	Temperature of half-decomposition, °C	Activation energy E_a, kJ/mol	Frequency factor Z, s^{-1}	Entropy change $\Delta S^{\#}$, J mol^{-1} K^{-1}	Free energy change $\Delta G^{\#}$, kJ/mol
L	303	18.16	7.63×10^{-3}	263.47	184.37
$[Mn(L)Cl{\cdot}H_2O]_2$	304	24.17	4.61×10^{-2}	241.53	150.46
$[Co(L)Cl{\cdot}H_2O]_2$	386	21.04	3.36×10^{-3}	234.48	174.43
$[Ni(L)Cl{\cdot}2H_2O]$	348	19.27	3.15×10^{-2}	255.63	164.68
$[Cu(L)]Cl_2$	414	26.17	2.59×10^{-2}	229.47	185.43
$[Ti(L)Cl_2{\cdot}H_2O]$	372	26.16	4.16×10^{-3}	256.39	194.54
$[Cr(L)Cl_2{\cdot}H_2O]$	408	20.38	3.18×10^{-3}	208.35	176.77
$[Fe(L)Cl_2{\cdot}H_2O]$	316	21.36	5.15×10^{-3}	217.26	165.70
$[Zr(OH)_3(L)CH_3OH]$	366	24.53	3.15×10^{-2}	183.57	188.64
$[UO_2(L)CH_3OH]NO_3$	384	23.44	3.17×10^{-3}	192.11	157.87

the coordinated ligand. The high-temperature residue was the corresponding metal oxide [the observed/calculated mass loss: 19.94/19.62 (Mn_3O_4); 21.32/20.44 (Co_3O_4); 18.66/18.19 (NiO); 21.87/21.46 (CuO); 19.26/19.14 (TiO_2); 18.19/18.04 (Cr_2O_3); 18.89/18.78 (Fe_2O_3); 27.30/25.14 (ZrO_2); and 43.85/43.46 (U_3O_8) wt %]. The thermal stability of the studied complexes (as determined by the temperature of the 50% degree of decomposition, Table 2 followed the Cu(II) > Cr(III) > Co(II) > UO_2^{2+} > Ti(III) > Zr(IV) > Ni(II) > Fe(III) > Mn(II) > free ligand series.

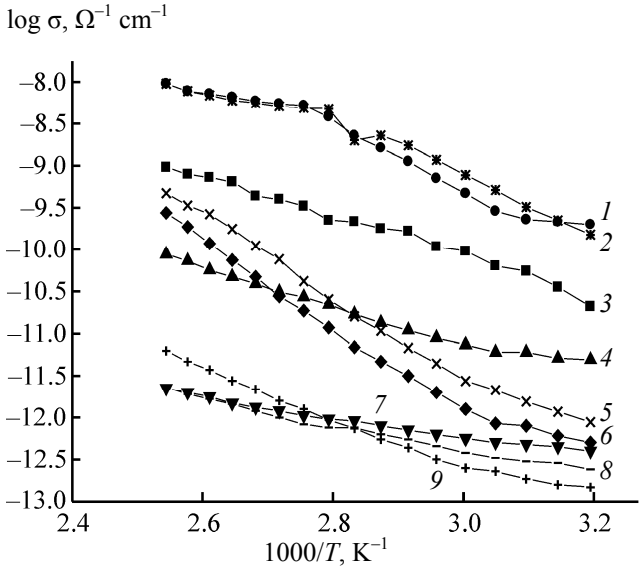

Fig. 2. Electrical conductivity of the complexes as function of temperature. (*1*) Ni(II), (*2*) Zr(IV), (*3*) Mn(II), (*4*) Co(II), (*5*) Fe(III), (*6*) Ti(III), (*7*) Cu(II), (*8*) UO_2(VI), and (*9*) Cr(III).

The Horowitz–Metzger method [26] was used to determine the kinetic parameters of the compounds thermal decomposition. The negative values of $\Delta S^{\#}$ suggested the higher ordered activated state that might be formed via chemisorption of oxygen and/or decomposition products. No definite trend in the E_a values (ranging in between 18.16 and 26.17 kJ/mol) was observed.

The solid-state d.c. electrical conductivity of the complexes in the form of the compressed pellets (Table 1) increased with temperature following the Arrhenius equation [27] (Fig. 2); the corresponding activation energy values are given in Table 1 as well. The increase in the conductivity started when charge carriers had gained enough of the energy to overcome the activation barrier; that reflected the property of a typical semiconductor [27]. The electrical conductivity of the complexes ranged in between 1.20×10^{-12} and 5.88×10^{-9} Ω^{-1} cm^{-1}, and the values measured at 373 K followed the Co > Zr > Mn > Fe > Ti > Ni > Cr > Cu > UO_2 series.

The ligand and its metal complexes were screened for the antibacterial activity against *E. coli, S. typhi, P. aeruginosa*, and *S. aureus*; DMSO was taken as reference. The results showed that the ligand exhibited the larger inhibition zone against *E. coli* and *P. aeruginosa*. All the complexes except for those of

Mn(II) and Co(II) possessed fairly good antibacterial activity against *E. coli*. The Fe(III) and Zr(IV) complexes showed good activity against *S. typhi*as as compared to the other complexes. The Ti(III) and uranyl complexes showed the smaller zone of inhibition against *P. aeruginosa*. The Cu(II) and Zr(IV) complexes exhibited enhanced activity towards *S. aureus*.

In general, the results revealed that the ligand antibacterial activity was enhanced after complexation with the metal ions. According to the Tweedy's chelation theory [28], the chelation reduces the polarity of the compound mainly owing to the partial sharing of the metal positive charge with the donor groups as well as possible π-electron density delocalization over the aromatic ring [29, 30]. This increases the lipophilic character of the metal chelate and favors its permeation through the lipid layer of a bacterial membrane. Hence, the enhancement of the ligand antibacterial activity upon the chelation was assigned to the increased lipophilic character of the complexes. As expected, the toxicity was increased at higher concentration of the complexes.

EXPERIMENTAL

All the chemicals and solvents used were of analytical grade. The metal salts [manganese(II) acetate dihydrate, anhydrous ferric chloride, cobalt(II) acetate dihydrate, nickel(II) acetate dihydrate, copper(II) acetate dihydrate, titanium(IV) chloride, chromium(III) chloride hexahydrate, zirconyl oxychloride octahydrate, and uranyl acetate dihydrate] were commercial products and were used as received.

2-Hydroxy[2-oxo-1,2-dihydro-3*H*-indol-3-ylidene]-benzohydrazide (L). A solution of 1*H*-indole-2,3-dione (isatin) (2.94 g, 0.02 mol) in methanol (20 mL) was added to a hot solution of salicylic hydrazide (3.04 g, 0.02 mol) in hot methanol (20 mL) upon stirring (Scheme 1). The mixture was heated using a water bath during 3–4 h. After cooling to ambient, the orange-colored solid was filtered, washed with methanol and diethyl ether, recrystallized from hot DMF, and dried in vacuum. Yield 70%, mp 303°C. ^{1}H NMR spectrum, δ, ppm: 6.7–7.5 m (8H, H_{Ar}), 10.4 s (1H, NH, ring), 11.3 s (1H, NH), 12.14 s (1H, OH).

Synthesis of complexes. Equimolar amounts of the corresponding metal salt and the ligand were dissolved in a minimal volume of hot methanol and DMF, respectively. The hot solutions were filtered and mixed upon continuous stirring. The reaction mixture was then digested on a sand bath.

In the case of Zr(IV) complexes, zirconyl oxychloride octahydrate (0.64 g, 0.002 mol) was dissolved in methanol (15 mL), a methanolic solution of anhydrous sodium acetate (0.32 g, 0.004 ml in 15 mL) was added, and the mixture was stirred during 5 min. The precipitated sodium chloride was filtered off. The ligand was dissolved in a minimal volume of hot DMF; the solution containing oxozirconium(IV) diacetate was added upon continuous stirring, and the mixture was refluxed on a sand bath. The colored precipitate was filtered off and washed sequentially with methanol, DMF, and petroleum ether. The product was dried in air at room temperature and stored in desiccators over $CaCl_2$. Yield 60–75%.

Microanalysis of carbon, hydrogen, and nitrogen content was performed using a Carlo Erba 1108 C-H-N-S analyzer. Infrared spectra of the ligand and the complexes (4000–400 cm^{-1}, KBr pellets) were recorded using a Perkin-Elmer-RX-I spectrophotometer. ^{1}H NMR spectrum (a solution of the ligand in a mixture of deuterated chloroform and DMSO) was recorded using a Bruker DRX-300 NMR spectrophotometer with TMS as internal reference. Magnetic susceptibility of the metal complexes was measured via the Gouy method at room temperature using $Hg[Co(SCN)_4]$ as the reference. Thermogravimetric analysis was performed using a manually operated

Scheme 1.

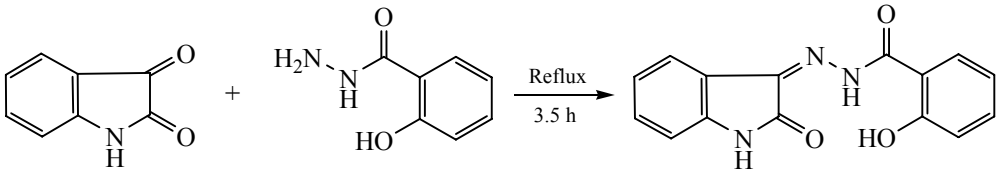

Isatin — Salicyl hydrazide — 2-Hydroxy[2-oxo-1,2-dihydro-3*H*-indol-3-ylidene]-benzohydrazide

thermobalance set up (specimen mass of 50–60 mg, heating up to 700°C at 10 deg/min, air atmosphere; copper(II) sulfate pentahydrate was measured under the same conditions for calibration purpose). The solid state d.c. electrical conductivity was measured as function of temperature (ambient to 403 K) with a micro voltmeter using the voltage drop method. The antibacterial activity against *E. coli*, *S. typhi*, *P. aeruginosa*, and *S. aureus* bacterial strains was measured via the disc diffusion method [28]. Nutrient agar and nutrient broth were used as the media. The plates were inoculated with the 24 h cultures. The compounds were tested at concentration of 500 ppm in DMSO; the solutions prepared were soaked with Whatmann filter paper no. 1 paper disc (10 mm in diameter). The discs were incubated on the previously seeded Petri dishes at 37°C during 24 h. The diameter of the zone of inhibition was measured in millimeter. DMSO was used as the blank.

REFERENCES

1. Qingbao, S., Xiaoli, W., Yongmin, L., and Yongxiang, M.A., *Polyhedron*, 1994, vol. 13, p. 2395. DOI: 10.1016/S0277-5387(00)88130-9.
2. Kumar, S., Dhar, D.N., and Saxena, P.N., *J. Sci. Ind. Res*., 2009, vol. 68, no. 3, p. 181.
3. Asadi, M., Sepehrpour, H., and Mohammadi, K., *J. Serb. Chem. Soc.,* 2011, vol. 76, p. 63.
4. Shibuya, Y., Nabari, K., Kondo, M., et al., *Chem. Lett.*, 2008, vol. 37, no. 1, p. 78.
5. Aslam, S.N., Stevenson, P.C., Kokubun, T., and Hall, D.R., *Microbiol. Res.,* 2009, vol. 164, no. 2, p. 191.
6. Abdel-Wahab, B.F., Abdel-Aziz, H.A., and Ahmed, E.M., *Eur. J. Med. Chem*., 2009, vol. 44, no. 6, p. 2632.
7. Murali Krishna, P., Hussain Reddy, K., Pandey, J.P., and Dayananda, S., *Trans. Metal Chem.,* 2008, vol. 33, no. 5, p. 661.
8. Boghaei, D.M., Sabouncheib, S.J.S., and Rayatib, S., *Synth. React. Inorg. Met. Org. Chem.,* 2000, vol. 30, p. 1535.
9. Raman, N., Sakthivel, A., Raja, J.D., and Rajasekaran, K., *Russ. J. Inorg. Chem.,* 2008, vol. 53, p. 213.
10. Nag, J.K., Pal, S., and Sinha, C., *Trans. Met. Chem*., 2005, vol. 30, p. 523.
11. Maurya, M.R., Singh, D.P., and Varma, S.K., *Synth. React. Inorg. Met. Org. Chem.,* 1989, vol. 19, p. 923.
12. Singh, R.V., Joshi, S.C., and Dwivedi, R., *Phosphorus Sulfur, Silicon, Relat. Elem.,* 2004, vol. 179, p. 227.
13. Aurel, P., Doina, H., Lonel, H., and Catalin, T., *Rev. Roumaine de Chime,* 2008, vol. 53, no. 3, p. 177.
14. Chandra, S., Verma, S., and Meera, P., *J. Ind. Chem. Soc*., 2008, vol. 85, p. 896.
15. Maldhure, A.K. and Aswar, A.S., *J. Ind. Chem. Soc.,* 2009, vol. 86, p. 697.
16. Joseph, A., Joseph, B., and Narayana, B., *J. Ind. Chem. Soc.,* 2008, vol. 85, p. 479.
17. Badwaik, V.B. and Aswar, A.S., *Russ. J. Inorg. Chem*., 2009, vol. 54, p. 1611.
18. Patel, M.N., Patel, J.R., and Sutaria, D.H., *Synth. React. Inorg. Met.-Org. Chem*., 1995, vol. 25, no. 5, p. 797.
19. Lee, J.D., *Concise Inorganic Chemistry*, London: Elbs, 1991, 4 ed.
20. Nejo, A.A., Kolawole, G.A., Opoku, A.R., Wolowska, J., and Brien, P.O., *Inorg. Chim. Acta,* 2009, vol. 362, p. 3993.
21. Grisenti, D.L., Smith, M.B., Fang, L., Bishop, N., and Wagenknecnt, P.S., *Inorg. Chim. Acta,* 2010, vol. 363, p. 157.
22. Dubey, R.K., Dubey, U.K., and Mishra, C.M., *Ind. J. Chem. A,* 2008, vol. 47, p. 1208.
23. Duelund, L., Hazell, R., Mckenzie, C.J., and Nielse, L.P., *J. Chem. Soc. Dalton Trans.,* 2001, vol. 152, p. 152.
24. Kumar, D., Syamal, A., and Singh, A.K., *Ind. J. Chem. A,* 2013, vol. 42, p. 280.
25. Chaudhary, R.G., Juneja, H.D., and Gharpure, M.P., *J. Therm. Anal. Calorim.,* 2013, vol. 112, p. 637.
26. Horowitz, H.H. and Metzger, M., *Anal. Chem*., 1963, vol. 35, p. 1464.
27. Modi, C.K., Patel, I.A., and Thaker, B.T., *J. Coord. Chem.,* 2008, vol. 61, p. 3110.
28. Tweedy, B.G., *Phytopathology*, 1964, vol. 55, p. 910.
29. Halli, M.B., Shashidhar, Z., and Quresi, S., *Synth. React. Inorg. Met.-Org. Chem*., 2004, vol. 34, no. 10, p. 1755.
30. Shivakumar, K., Vittalareddy, S.P., and Halli, M.B., *J. Coord. Chem.,* 2008, vol. 61, no. 14, p. 2274.